



# MIT Open Access Articles

## *Pair superfluid and supersolid of correlated hard-core bosons on a triangular lattice*

The MIT Faculty has made this article openly available. **Please share** how this access benefits you. Your story matters.

<b>Citation</b>	Jiang, Hong-Chen, Liang Fu, and Cenke Xu. "Pair Superfluid and Supersolid of Correlated Hard-core Bosons on a Triangular Lattice." <i>Physical Review B</i> 86.4 (2012). ©2012 American Physical Society
<b>As Published</b>	<a href="http://dx.doi.org/10.1103/PhysRevB.86.045129">http://dx.doi.org/10.1103/PhysRevB.86.045129</a>
<b>Publisher</b>	American Physical Society
<b>Version</b>	Final published version
<b>Accessed</b>	Wed Dec 13 19:36:30 EST 2017
<b>Citable Link</b>	<a href="http://hdl.handle.net/1721.1/73871">http://hdl.handle.net/1721.1/73871</a>
<b>Terms of Use</b>	Article is made available in accordance with the publisher's policy and may be subject to US copyright law. Please refer to the publisher's site for terms of use.
<b>Detailed Terms</b>	

# Pair superfluid and supersolid of correlated hard-core bosons on a triangular lattice

Hong-Chen Jiang

*Kavli Institute for Theoretical Physics, University of California, Santa Barbara, California 93106, USA and  
Center for Quantum Information, IIIS, Tsinghua University, Beijing 100084, China*

Liang Fu

*Department of Physics, Massachusetts Institute of Technology, Cambridge, Massachusetts 02139, USA*

Cenke Xu

*Department of Physics, University of California, Santa Barbara, California 93106, USA*

(Received 15 April 2012; published 24 July 2012)

We have systematically studied the hard-core Bose-Hubbard model with correlated hopping on a triangular lattice using the density-matrix renormalization group method. A rich ground-state phase diagram is determined. In this phase diagram there is a supersolid phase and a pair superfluid phase due to the interplay between the ordinary frustrated boson hopping and an unusual correlated hopping. In particular, we find that the quantum phase transition between the supersolid phase and the pair superfluid phase is continuous.

DOI: [10.1103/PhysRevB.86.045129](https://doi.org/10.1103/PhysRevB.86.045129)

PACS number(s): 67.80.kb, 67.85.Bc, 67.85.De, 03.75.Lm

## I. INTRODUCTION

The Bose-Hubbard model, as the first explicit example of quantum phase transition, has been studied extensively with many techniques. The simplest version of the Bose-Hubbard model only involves a Mott insulator phase and a superfluid phase,<sup>1</sup> and the quantum phase transition between these two phases can be well described by a semiclassical Landau-Ginzburg theory. For example, in two dimensions, this quantum phase transition is either an ordinary three-dimensional (3D)  $XY$  transition or a  $z = 2$  mean-field transition depending on the chemical potential. In the last few years, it was proposed that various extended Bose-Hubbard models can have much richer and more exotic behaviors. For example, a  $Z_2$  topological liquid phase has been discovered in an extended Bose-Hubbard model on the kagome lattice,<sup>2-5</sup> and in the same model an exotic quantum phase transition between the  $Z_2$  liquid and a conventional superfluid phase was identified.<sup>6</sup> Also, with an extra ring exchange term, it was demonstrated both numerically and analytically that the Bose-Hubbard model can have an exotic fractionalized Bose metal phase.<sup>7-9</sup>

With a hard core constraint, (i.e., doubly occupied sites are removed from the Hilbert space) the Bose-Hubbard model is equivalent to a spin-1/2 model. Due to the rapid development of numerical techniques, exotic phases have been identified in many quantum spin-1/2 models as well. For example, based on the density-matrix renormalization group (DMRG) method, a fully gapped topological liquid phase has been discovered in the kagome lattice spin-1/2 Heisenberg model,<sup>10,11</sup> as well as the  $J_1$ - $J_2$  Heisenberg model on the square lattice.<sup>12</sup>

In this paper, using the DMRG method, we demonstrate that in one simple extended hard-core Bose-Hubbard model there are three different interesting phenomena. First of all, there is a supersolid (SS) phase, where there is a coexistence of the off-diagonal long-range order of the boson creation operator and a boson density wave order. Second, there is a pair superfluid (PSF) phase, where  $\langle b_i \rangle = 0$  while  $\langle b_i b_{i+\alpha} \rangle \neq 0$ . This pair superfluid phase is an analog of the charge- $4e$  superconductor

that was discussed recently.<sup>13-15</sup> Third, we show that there is a continuous quantum phase transition between the supersolid and the pair superfluid phase.

## II. MODEL HAMILTONIAN

We consider a hard-core Bose-Hubbard model with a correlated hopping on a triangular lattice

$$H = t \sum_{\langle ij \rangle} (b_i^\dagger b_j + \text{H.c.}) + V \sum_{\langle ij \rangle} n_i n_j - K \sum_{ijk \in \Delta} (n_i b_j^\dagger b_k + \text{H.c.}), \quad (1)$$

where  $b_i^\dagger$  ( $b_i$ ) is the boson creation (annihilation) operator and  $n_i$  is the boson number operator on site  $i$ . In this Hamiltonian  $t$  is the ordinary nearest-neighbor (NN) boson hopping amplitude, and  $V$  is the NN repulsive interaction.  $K$  is a correlated hopping term and  $ijk \in \Delta$  are three sites in a small triangle (shown in Fig. 1) of the lattice. We will see that the presence of the  $K$  term significantly enriches the phase diagram of this model. In the numerical simulations, for simplicity, we will always set  $t = 1$  as the unit of energy, and focus on the case with  $V > 0$  and  $K > 0$ . Notice that here the boson hopping term is frustrated. It has been proposed that the correlated hopping terms can be realized in cold atom systems trapped in an optical lattice.<sup>16</sup>

We determine the ground-state phase diagram of the model Hamiltonian Eq. (1) by extensive and highly accurate DMRG<sup>17,18</sup> simulations. In particular, we consider a system with the total number of sites  $N = L_x \times L_y$ , which are spanned by multiples  $L_x \hat{x}$  and  $L_y \hat{y}$  of the unit vectors  $\hat{x} = (1, 0)$  and  $\hat{y} = (\frac{1}{2}, \frac{\sqrt{3}}{2})$ . For the DMRG calculation, we consider both a cylinder boundary condition (CBC) and a fully periodic boundary condition. Here, CBC means the open boundary condition along the  $L_x$  direction, while the periodic boundary condition is along the  $L_y$  direction. This allows us to work on numerous cylinders with a much larger system size to

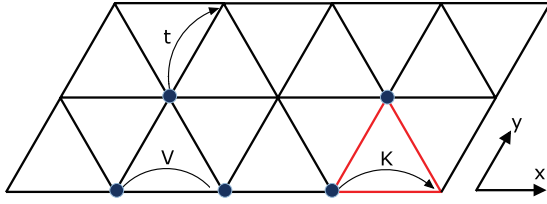


FIG. 1. (Color online) Illustration of the three-leg ladder geometry with unit vectors  $\hat{x} = (1,0)$  and  $\hat{y} = (\frac{1}{2}, \frac{\sqrt{3}}{2})$ . The boson hopping strength is  $t$ , and the repulsive interaction is  $V$ . The correlated hopping term  $K$  moves a hard-core boson from one site to another one, depending on the number of bosons in the third site in the same small triangle.

reduce the finite-size effect for a more reliable extrapolation to the thermodynamic limit. We keep more than  $m = 6000$  states in each DMRG block for most systems, which is found to give excellent convergence with the tiny truncation errors that can be fully neglected.

### III. PHASE DIAGRAM

The main result of this paper is illustrated in the phase diagram of the model [Eq. (1)] at filling  $\rho = \frac{1}{6}$ , as shown in Fig. 2, obtained by extensive DMRG studies on numerous cylinders with  $L_y = 3-9$ . The nature of the ground state of the model Hamiltonian Eq. (1) at half filling has already been studied previously without considering the correlated hopping term  $K$ , where a supersolid phase was found to be stable over a wide range of the interaction strength.<sup>19-21</sup> In the SS phase there is a long-range order of both the boson creation operator and the boson density wave. Further study<sup>22</sup> shows that this SS phase will also survive at low boson density, such as  $\rho = \frac{1}{6}$ , when the repulsive interaction is strong enough. For weak interaction, this SS phase will give way to the simple atomic superfluid phase.

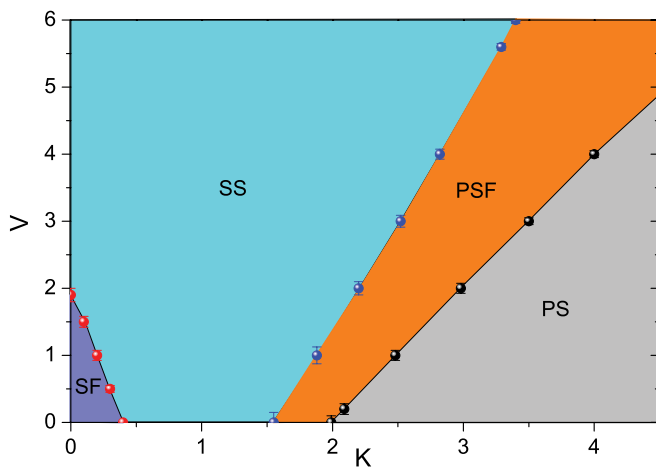


FIG. 2. (Color online) Ground-state phase diagram for the correlated hard-core Bose-Hubbard model [Eq. (1)] in a triangular lattice at filling  $\rho = 1/6$ , as determined by accurate DMRG calculations on cylinders with  $L_y$  up to 9. Changing the coupling parameters  $V$  and  $K$ , four different phases are found, including the superfluid (SF), supersolid (SS), pair superfluid (PSF), and the phase separation (PS).

In our current paper, we demonstrate that the unfrustrated correlated hopping term will compete with the repulsive interaction and lead to an interesting phase diagram. In particular, with the intermediate strength of  $K$ , the SS phase is driven into a uniform pair superfluid phase where  $\langle b_i \rangle = 0$ , while  $\langle b_i b_{i+\alpha} \rangle \neq 0$ .

To analyze the ground-state properties of the system, we calculate both the boson density structure factor

$$S(\mathbf{k}) = \frac{1}{N} \sum_{ij} e^{i\mathbf{k} \cdot (\mathbf{r}_i - \mathbf{r}_j)} \langle (n_i - \rho)(n_j - \rho) \rangle, \quad (2)$$

and the momentum distribution function

$$M_b(\mathbf{k}) = \frac{1}{N} \sum_{ij} e^{i\mathbf{k} \cdot (\mathbf{r}_i - \mathbf{r}_j)} \langle b_i^+ b_j \rangle, \quad (3)$$

where  $\rho$  is the filling factor of the system. We also calculate the pair superfluid structure factor

$$M_p^\alpha(\mathbf{k}) = \frac{1}{N} \sum_{ij} e^{i\mathbf{k} \cdot (\mathbf{r}_i - \mathbf{r}_j)} \langle \Delta_i^{+\alpha} \Delta_j^\alpha \rangle, \quad (4)$$

to characterize the pair superfluid phase. Here  $\Delta_i^\alpha = b_i b_{i+\alpha}$  is the nearest-neighbor pair annihilation operator along the  $\alpha$  direction, with  $\alpha = \hat{x}, \hat{y}$  or  $\hat{y} - \hat{x}$ .

In both the SF phase and supersolid phase, the obtained  $S(\mathbf{k})$  and  $M_b(\mathbf{k})$  show Bragg peaks at the corners of the hexagonal Brillouin zone [e.g., at  $k_1 = (\pm 4\pi/3, 0)$ ]. On the other hand,  $M_p^\alpha(\mathbf{k})$  shows peaks at zero momentum [i.e.,  $k_0 = (0,0)$  in the whole phase diagram except the phase separation]. In particular, at small  $K$ , both the peak of the boson density structure factor  $S(\mathbf{k})$  and the momentum distribution function  $M(\mathbf{k})$  are very sharp, as shown in Fig. 3. Here the peak position in Fig. 3 ( $k_x = 4\pi/3, k_y = 2\pi/3$ ) corresponds to  $k_1 = (4\pi/3, 0)$  of the hexagonal Brillouin zone. One can obtain the corresponding order parameters in the thermodynamic limit based on the finite-size scaling of the peak values  $S(k_1)$ ,  $M_b(k_1)$ , and  $M_p^\alpha(k_0)$ . Specifically, the boson density wave order parameter and the boson condensate density can be determined by  $m_s = S(k_1)/N$  and  $C_b = M_b(k_1)/N$ , respectively, while the total pair condensate density is given by  $C_p = \sum_\alpha C_p^\alpha = \sum_\alpha M_p^\alpha(k_0)/N$ . Examples of these order parameters are shown in Fig. 4 as a function of correlated hopping  $K$  with  $N = 12 \times 6, 12 \times 9$  and  $18 \times 9$ . At large  $V = 6.0$ , with the increase of  $K$ ,  $m_s$  decreases continuously, while  $C_b$  increases at first and then decreases with larger  $K$ .

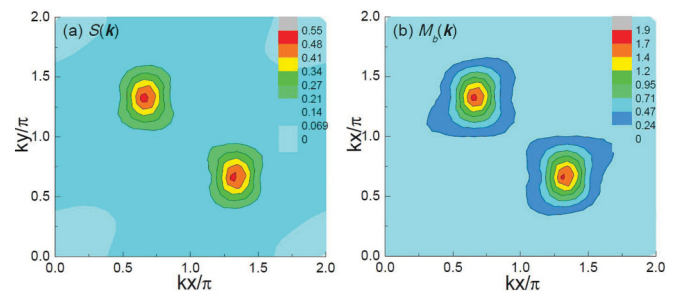


FIG. 3. (Color online) Examples of the contour plot of the boson density structure factor  $S(\mathbf{k})$  and boson momentum distribution  $M_b(\mathbf{k})$  as a function of  $\mathbf{k}$ , at  $V = 6.0$  and  $K = 1.0$  for system  $N = 12 \times 6$ .

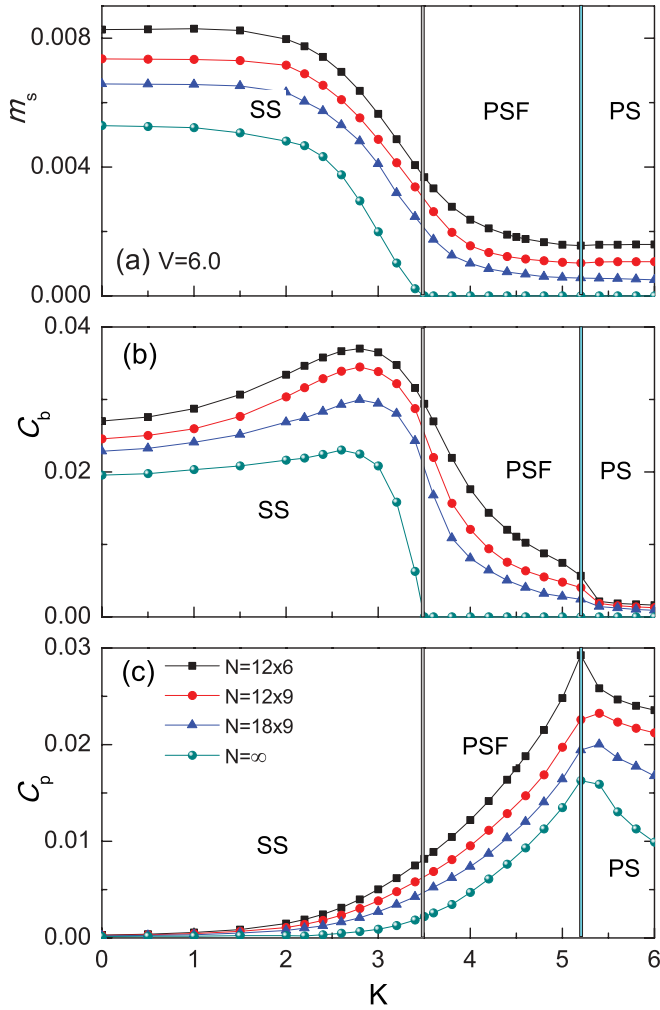


FIG. 4. (Color online) (a) The density structure factor order parameter  $m_s$ , (b) atomic condensate density  $C_b$  at momentum  $k_1 = (4\pi/3, 0)$ , and (c) pair condensate density  $C_p$  at momentum  $k_0 = (0, 0)$ , as functions of  $K$  at  $V = 6.0$  and filling  $\rho = 1/6$ , respectively, with system size  $N = 12 \times 6$ ,  $12 \times 9$ ,  $18 \times 9$ , and the corresponding extrapolations in the thermodynamic limit.

Eventually both  $m_s$  and  $C_b$  become very weak beyond a certain critical value of  $K$ . On the other hand,  $C_p$  increases with  $K$  monotonically before phase separation.

Nonzero  $m_s$  and  $C_b$  in the thermodynamic limit correspond to the diagonal long-range order (LRO) and off-diagonal long-range order (ODLRO), respectively. Examples of the finite-size scaling are shown in Fig. 5 by plotting  $m_s$ ,  $C_b$ , and  $C_p$  as functions of  $1/N$ , at  $V = 6.0$  and different  $K$ , using quasi-two-dimensional (2D) lattice geometry with system size up to  $N = 18 \times 9$ . The obtained order parameters extrapolated to the thermodynamic limit are presented in Figs. 4 (dark cyan sphere) and 5. It is worth noting that after extrapolation both  $m_s$  and  $C_b$  continuously decrease to zero simultaneously at the critical  $K$ , and the system enters the pair superfluid phase in the thermodynamic limit, indicating a continuous phase transition. However,  $C_p$  is nonzero in both the SS and PSF, and it always increases monotonically with  $K$  [see Fig. 4(c)] before phase separation. Specifically, the finite-size scaling for  $C_p$  at  $K = 2.0$  in the supersolid phase gives us a small but finite

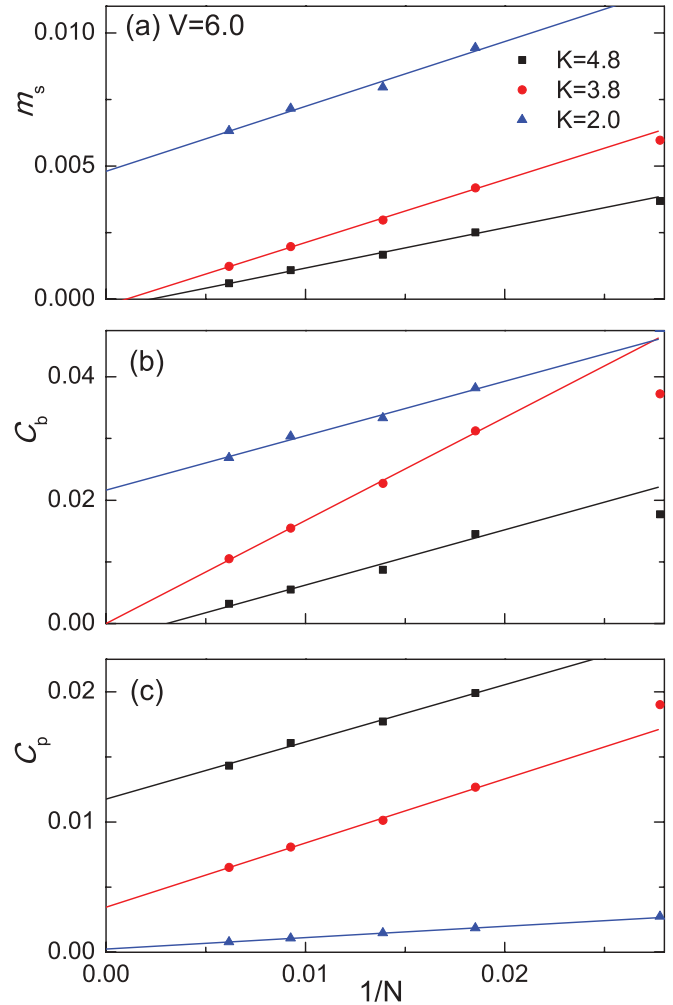


FIG. 5. (Color online) Examples of finite-size scaling of (a) the density structure factor order parameter  $m_s$  and (b) atomic condensate density  $C_b$  at momentum  $k_1 = (4\pi/3, 0)$ , as well as (c) the pair condensate density  $C_p$  at momentum  $k_0 = (0, 0)$ , for different  $K$  at  $V = 6.0$  and filling  $\rho = 1/6$ , with system size up to  $18 \times 9$ .

value  $C_p \approx 2.5(3) \times 10^{-4}$  within the numerical error (around 2% of  $C_p$  at  $K = 4.8$ ), as shown in Fig. 5(c).

With the decrease of the repulsive interaction  $V$ , both the supersolid phase and pair superfluid phase become weaker and move to smaller  $K$ . In particular, a superfluid phase appears at small  $K$  locating at the left bottom corner in the phase diagram (see Fig. 2). Compared with the supersolid and pair superfluid phase at large  $V$ , the pair condensate density at  $k_0 = (0, 0)$  becomes zero [i.e.,  $C_p(k_0) = 0$ ]. Even with the absence of the repulsive interaction  $V$ , the atomic superfluid phase is completely suppressed with the increase of  $K$  and gives way to the supersolid phase through a first-order transition around  $K = 0.3$ . This can be seen clearly in Fig. 6, in which  $m_s$  and  $C_p$  jump from zero to a finite value in the thermodynamic limit, while  $C_b$  encounters a sharp drop to a smaller but still finite value. It is interesting to note that the pair superfluid phase still remains robust in a finite parameter region  $K \approx 1.6-2.0$ , even in the absence of the repulsive interaction  $V$ , due to the competition between  $t$  and  $K$ . Finally, the system becomes phase separated when  $K$  becomes dominant.

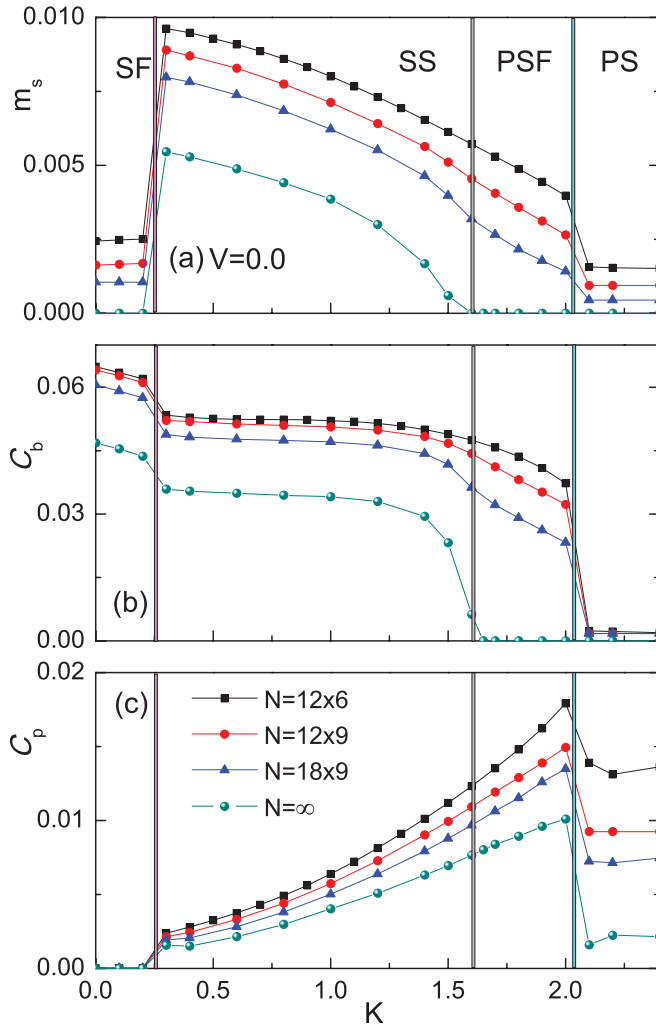


FIG. 6. (Color online) (a) The density structure factor order parameter  $m_s$ , (b) atomic condensate density  $C_b$  at momentum  $k_1 = (4\pi/3, 0)$ , and (c) the pair condensate density  $C_p$  at momentum  $k_0 = (0, 0)$ , as functions of  $K$  at  $V = 0.0$  and filling  $\rho = 1/6$ , respectively, with system size  $N = 12 \times 6$ ,  $12 \times 9$ , and  $18 \times 9$ , as well as the corresponding extrapolations in the thermodynamic limit.

#### IV. THEORETICAL UNDERSTANDING

In this section, we develop a simple Landau-Ginzburg theory to describe the supersolid, superfluid, and paired superfluid phases on the triangle lattice, including the phase transitions between them. The dispersion of a boson with frustrated hopping in a triangular lattice has two minima at  $\vec{K}$  and  $-\vec{K}$ , where  $\vec{K} = (4\pi/3, 0)$ . Therefore we introduce the two  $U(1)$  order parameters  $\phi_{1,2}$  for boson condensate at  $\pm\vec{K}$

$$b^\dagger(\vec{x}) \sim \phi_1(\vec{x})e^{i\vec{K}\cdot\vec{x}} + \phi_2(\vec{x})e^{-i\vec{K}\cdot\vec{x}}. \quad (5)$$

Under time reversal and lattice symmetries,  $\phi_{1,2}$  transform as follows:

$$\begin{aligned} T_i &: \phi_1 \rightarrow \phi_1 e^{-i2\pi/3}, \quad \phi_2 \rightarrow \phi_2 e^{i2\pi/3}, \quad i = 1, 2, 3, \\ C_6 &: \phi_1 \rightarrow \phi_2, \quad \phi_2 \rightarrow \phi_1, \\ M_x &: \phi_1 \rightarrow \phi_2, \quad \phi_2 \rightarrow \phi_1, \end{aligned}$$

$$\begin{aligned} \Theta &: \phi_1 \rightarrow \phi_2, \quad \phi_2 \rightarrow \phi_1, \\ U(1) &: \phi_1 \rightarrow \phi_1 e^{i\theta}, \quad \phi_2 \rightarrow \phi_2 e^{i\theta}. \end{aligned} \quad (6)$$

Here  $T_i$  are translations by the three unit vector  $\mathbf{a}_i$  of the triangle lattice  $\mathbf{a}_1 = (1, 0)$ ,  $\mathbf{a}_2 = (-1/2, \sqrt{3}/2)$ ,  $\mathbf{a}_3 = (-1/2, -\sqrt{3}/2)$ .  $C_6$  is  $\pi/3$  rotation.  $M_x$  is reflection about the  $x$  axis.  $\Theta$  is the time-reversal transformation.  $U(1)$  is the global phase transformation.

The supersolid phase is characterized by *two* nonzero condensate order parameters  $\phi_1$  and  $\phi_2$ , which have momentum  $\vec{K}$  and  $-\vec{K}$ , respectively. The coexistence of these two superfluid orders necessarily induces a nonzero density wave order  $\rho \sim \phi_1^* \phi_2$  at momentum  $2\vec{K} = -\vec{K}$ , where we have used the fact that  $3\vec{K} = 0$  up to a reciprocal lattice vector in the triangular lattice. The presence of both superfluid and density-wave order taken together signals a supersolid phase, as we found numerically. On the other hand, the paired superfluid phase is characterized by a nonzero pair condensate order parameter  $\Delta$  at zero momentum, whereas both  $\phi_1$  and  $\phi_2$  are disordered.

Since the supersolid phase has a lower symmetry than the paired superfluid phase, the phase transition can be understood as the development of the long-range single boson superfluid in the paired superfluid (disordered) phase within the framework of the Landau-Ginzburg theory in  $2 + 1$  dimensions. The effective Landau-Ginzburg Lagrangian, whose form is dictated by the symmetry property (6), is given by

$$\begin{aligned} \mathcal{L} = & \frac{r}{2}(\phi_1^* \phi_1 + \phi_2^* \phi_2) - (\Delta \phi_1^* \phi_2^* + \Delta^* \phi_1 \phi_2) \\ & + u(|\phi_1|^4 + |\phi_2|^4) + 2u_{12}|\phi_1|^2|\phi_2|^2 + v(\phi_1^{*3}\phi_2^3 + \phi_1^3\phi_2^{*3}). \end{aligned}$$

As  $r$  decreases,  $\phi_1$  and  $\phi_2$  become nonzero, which signals the onset of superfluid order as well as the associated density wave order  $\phi_1^* \phi_2$ . Note that the pair order parameter  $\Delta$  is nonzero across the transition. Without loss of generality,  $\Delta$  is chosen to be real and positive. Due to the trilinear coupling term between  $\Delta$ ,  $\phi_1$ , and  $\phi_2$ ,  $\mathcal{L}$  is minimized by  $\phi_2^* = \phi_1 \equiv \phi$ , where  $\phi$  is *complex*. The last term in  $S$  is symmetry allowed for the triangular lattice, and locks the relative phase between  $\phi_1$  and  $\phi_2$ , and pins the phase of  $\rho = \phi_1 \phi_2^* = \phi^2$  to three distinct values corresponding to three degenerate density wave patterns in the supersolid phase. In terms of  $\phi$ ,  $\mathcal{L}$  is given by

$$\mathcal{L} = |\partial_\mu \phi|^2 + r_1 |\phi|^2 + u' |\phi|^4 + v(\phi^6 + \phi^{*6}). \quad (7)$$

Except for the last term,  $\mathcal{L}$  is the standard complex scalar field theory in  $2 + 1$  dimensions, and this transition belongs to the 3D  $XY$  universality class with order parameter  $\phi$ . By power counting, the sixth-order phase-locking term is strongly irrelevant at the critical point, thus this transition is continuous.

Interestingly, the above  $XY$  transition differs from conventional paired to single boson superfluid transition, which lies in the Ising universality class. The distinction arises from the fact that the superfluid phase studied here has two coexisting (rather than one) condensate order parameters, of which the relative phase is a well defined physical quantity associated with the density wave order. Our theory can be directly tested by further numerical studies on the critical exponent for the physical order parameter at the quantum critical point. For example, the critical exponent  $\nu$  take the value of the ordinary 3D  $XY$  transition  $\nu \sim 0.67$ . Also, the density wave order

parameter  $\rho \sim \phi^2$  is a bilinear of  $\phi$  in Eq. (7), thus our theory predicts that the order parameter  $\rho$  has an anomalous dimension  $\eta \sim 1.49$ . These predictions can be verified by further numerical studies on the model in Eq. (1).

We can also interpret the supersolid to pair superfluid transition in terms of the topological defects inside the supersolid phase. For convenience, let us rewrite the fields  $\phi_1$  and  $\phi_2$  introduced in Eq. (5) as follows:

$$\phi_1 = \phi \psi, \quad \phi_2 = \phi^* \psi. \quad (8)$$

$\phi$  and  $\phi^*$  are complex fields that carry lattice momentum  $\vec{K}$  and  $-\vec{K}$ , respectively, while  $\psi$  carries the  $U(1)$  symmetry of the original boson operator  $b_i$ . Thus the boson density wave order parameter is  $\rho \sim \phi_1 \phi_2^* \sim \phi^2$ , and the pair superfluid order parameter is  $b_i b_{i+\alpha} \sim \phi_1 \phi_2 \sim \psi^2$ .

In Eq. (8), because  $\phi_1$  and  $\phi_2$  are both physical degrees of freedom,  $\phi$  and  $\psi$  are defined up to a  $Z_2$  gauge ambiguity (i.e., the physics is unchanged under the transformation  $\phi \rightarrow -\phi$ ,  $\psi \rightarrow -\psi$ ). The supersolid phase corresponds to the case where both  $\phi$  and  $\psi$  are condensed, while in the pair superfluid phase only  $\psi$  is condensed. Inside the supersolid phase, the smallest superfluid vortex has only  $\pi$  vorticity (i.e., it is a bound state between a  $\pi$  vortex of  $\psi$  and a  $\pi$  vortex of  $\phi$ ). In other words, both  $\psi$  and  $\phi$  will change sign after encircling this vortex, while the physical degree of freedom is unchanged. Notice that the  $\pi$  vortex of  $\phi$  is a full vortex of boson density wave order  $\rho$ , which is equivalent to a *dislocation* of the density wave pattern.

Starting with the supersolid phase, if we want to drive a transition into the pair superfluid phase, we need to “melt” the boson density wave order by condensing its defects. However, since the pair superfluid phase also has a half quantum  $\pi$  vortex, this transition cannot be driven by condensing the smallest  $\pi$  vortex discussed in the previous paragraph. Instead, it must be driven by the condensation of the  $2\pi$  vortex of  $\phi$ , which only melts the boson density wave, but leaves

the superfluid stiffness unaffected. Since the physical boson density wave order parameter  $\rho \sim \phi^2$  is a bilinear of  $\phi$ , this transition is driven by condensing a “double” dislocation of  $\rho$ . Thus this transition is analogous to the transition between the pair-density-wave and charge- $4e$  superconductors discussed in Ref. 13.

## V. SUMMARY AND EXTENSION

We have studied a hard-core Bose-Hubbard model with an unusual correlated hopping on a triangular lattice using the density-matrix renormalization group method. In the phase diagram, we discovered a supersolid phase and a pair superfluid phase, in addition to the standard superfluid phase. The supersolid and pair superfluid phases were discussed separately before in different spin models.<sup>19–25</sup> However, to our knowledge it is the first time that both these phases are realized in one model. We also theoretically establish that the phase transition between the supersolid phase and the pair superfluid phase is continuous.

If the phase coherence and superfluid stiffness of the pair superfluid phase are destroyed, then the system most likely enters a fully gapped  $Z_2$  liquid phase with the same topological order as the toric code model.<sup>26</sup> Presumably this new transition can be obtained by turning on some extra terms in the Hamiltonian. We will leave this to future study.

## ACKNOWLEDGMENTS

We would like to thank Matthew Fisher, Steve Kivelson, W. Vincent Liu, Senthil Todadri, and especially Leon Balents and Fa Wang for insightful discussions. This work was partially supported by the KITP NSF Grant No. PHY05-51164 and the NSF MRSEC Program under Award No. DMR 1121053, and the NBRPC (973 Program) 2011CBA00300 (2011CBA00302). Cenke Xu is supported by the Sloan Foundation. Liang Fu is supported by start-up funds of MIT.

<sup>1</sup>M. P. A. Fisher, P. B. Weichman, G. Grinstein, and D. S. Fisher, *Phys. Rev. B* **40**, 546 (1989).

<sup>2</sup>L. Balents, M. P. A. Fisher, and S. M. Girvin, *Phys. Rev. B* **65**, 224412 (2002).

<sup>3</sup>S. V. Isakov, Yong Baek Kim, and A. Paramekanti, *Phys. Rev. Lett.* **97**, 207204 (2006).

<sup>4</sup>S. V. Isakov, M. B. Hastings, and R. G. Melko, *Nat. Phys.* **7**, 772 (2011).

<sup>5</sup>T. Senthil and O. Motrunich, *Phys. Rev. B* **66**, 205104 (2002).

<sup>6</sup>S. V. Isakov, R. G. Melko, and M. B. Hastings, *Science* **335**, 193 (2012).

<sup>7</sup>M. S. Block, R. V. Mishmash, R. K. Kaul, D. N. Sheng, O. I. Motrunich, and M. P. A. Fisher, *Phys. Rev. Lett.* **106**, 046402 (2011).

<sup>8</sup>M. S. Block, D. N. Sheng, O. I. Motrunich, and M. P. A. Fisher, *Phys. Rev. Lett.* **106**, 157202 (2011).

<sup>9</sup>R. V. Mishmash, M. S. Block, R. K. Kaul, D. N. Sheng, O. I. Motrunich, and M. P. A. Fisher, *Phys. Rev. B* **84**, 245127 (2011).

<sup>10</sup>H. C. Jiang, Z. Y. Weng, and D. N. Sheng, *Phys. Rev. Lett.* **101**, 117203 (2008).

<sup>11</sup>S. Yan, D. A. Huse, and S. R. White, *Science* **332**, 1173 (2011).

<sup>12</sup>H.-C. Jiang, H. Yao, and L. Balents, *Phys. Rev. B* **86**, 024424 (2012).

<sup>13</sup>E. Berg, E. Fradkin, and S. A. Kivelson, *Nat. Phys.* **5**, 830 (2009).

<sup>14</sup>E. G. Moon, *Phys. Rev. B* **85**, 245123 (2012).

<sup>15</sup>E. V. Herland, E. Babaev, and A. Sudbø, *Phys. Rev. B* **82**, 134511 (2010).

<sup>16</sup>L. Mazza, M. Rizzi, M. Lewenstein, and J. I. Cirac, *Phys. Rev. A* **82**, 043629 (2010).

<sup>17</sup>S. R. White, *Phys. Rev. Lett.* **69**, 2863 (1992); **77**, 3633 (1996).

<sup>18</sup>E. M. Stoudenmire and S. R. White, *Annu. Rev. Condens. Matter Phys.* **3**, 111 (2012).

<sup>19</sup>R. G. Melko, A. Paramekanti, A. A. Burkov, A. Vishwanath, D. N. Sheng, and L. Balents, *Phys. Rev. Lett.* **95**, 127207 (2005).

<sup>20</sup>H. C. Jiang, M. Q. Weng, Z. Y. Weng, D. N. Sheng, and L. Balents, *Phys. Rev. B* **79**, 020409(R) (2009).

<sup>21</sup>F. Wang, F. Pollmann, and A. Vishwanath, *Phys. Rev. Lett.* **102**, 017203 (2009).

<sup>22</sup>H. C. Jiang *et al.* (in preparation).

<sup>23</sup>Lars Bonnes and Stefan Wessel, *Phys. Rev. Lett.* **106**, 185302 (2011).

<sup>24</sup>K. P. Schmidt, J. Dorier, A. Lauchli, and F. Mila, *Phys. Rev. B* **74**, 174508 (2006).

<sup>25</sup>K. P. Schmidt, J. Dorier, A. M. Lauchli, and F. Mila, *Phys. Rev. Lett.* **100**, 090401 (2008).

<sup>26</sup>A. Yu. Kitaev, *Ann. Phys. (NY)* **303**, 2 (2003).